

DIAGNOSTIC NUCLEAR MEDICINE

In Vivo Simulation of Thallium-201 Myocardial Scintigraphy by Seven-Pinhole Emission Tomography

David L. Williams, James L. Ritchie, George D. Harp, James H. Caldwell, and Glen W. Hamilton

Veterans Administration Medical Center, Seattle, Washington

Seven-pinhole emission tomography has been studied under conditions that simulate clinical myocardial imaging with thallium-201, and is compared with planar imaging with a heart phantom. The seven-pinhole technique produces reconstructed images that offer a tomographic presentation of the object but do not quantitatively represent true cross sections of the object's activity distribution. Tomography produces significantly greater image contrast than planar imaging, even when maximal background subtraction is used to enhance the planar images. Two quantitative limitations of seven-pinhole tomography are noted for a simulated 24-g, 1.5-cm-thick complete transmural infarct: (a) the defect's activity concentration is not accurately reconstructed, and (b) it propagates longitudinally into some reconstructed planes that do not contain it. The imaging limitations of seven-pinhole tomography under the conditions studied are shown to be consistent on several camera/computer/software configurations.

J Nucl Med 21: 821-828, 1980

Seven-pinhole tomography, as developed by Vogel et al. (1), is an emission imaging technique that calculates multiple slice reconstructions through an organ from a single multiprojection image. A special-purpose collimator containing seven pinholes is attached to a conventional wide-field-of-view scintillation camera and records simultaneous, nonoverlapping projections of a small organ (e.g., the heart) over a limited angle of  $\pm 26.5^\circ$ , and at six equally spaced angular intervals about the principal optic axis. The seven-view raw data, along with flood and point-source calibrations, are computer-processed by the simultaneous iterative reconstruction technique (SIRT) to obtain multiple image planes through the organ of interest (2). The reconstructed planes are parallel to the pinhole aperture plate. Thus, tomographic imaging of the myocardial distribution of thallium-201 in the LAO view produces reconstructed planes from apex to base, perpendicular to the long axis of the heart.

The collimator design has been optimized for imaging the myocardium (1). When applied to myocardial perfusion imaging, the seven-pinhole method has demonstrated improved detection sensitivity over conventional planar imaging for the diagnosis of coronary artery disease (1,3). The purpose of this report was to study the seven-pinhole method under controlled phantom conditions and compare it with conventional planar thallium imaging in the LAO view.

METHODS

A multichamber cardiac phantom (Fig. 1) was constructed following the design of Mueller et al. (4), who have previously reported the planar imaging limitations of thallium-201. The interior partitions of the phantom and their volumes are shown in Fig. 2. Each chamber was individually leak-tested with colored dye under pressure and its seams sealed with low-viscosity acrylic cement until the compartment was water tight. The wall thickness of all myocardial chambers was 1.5 cm. Apical and posterior chambers were azimuthally symmetric about a 150-cc central cavity simulating the left ventricle. The

Received Dec. 7, 1979; revision accepted May 6, 1980.

For reprints contact: David L. Williams, PhD, Nuclear Medicine Section (115), VA Medical Ctr, 4435 Beacon Ave. S., Seattle, WA 98108.



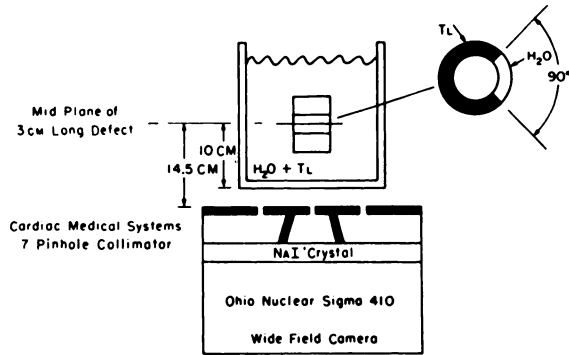


**FIG. 4.** Tomographic imaging configuration. Without changing conditions of "simulated" patient, phantom system was moved to wide-field camera with seven-pinhole tomographic collimation and placed so that apical activity projected just inside collimator's field of view on camera's persistence scope.

count images were taken on a nuclear medicine computer system to achieve 800 k total counts of raw data for reconstruction. A  $128 \times 128 \times 8$ -bit static image format was used for both phantom and calibration images. Sixteen-plane reconstructions were obtained by the commercial algorithm\* supplied with the collimator. The reconstructed planes encompassed the heart phantom from apex to base; their locations in object space with respect to the pinhole plane are given in Table 2. The reconstruction algorithm makes an approximate attenuation correction for the 80-keV x-rays of Tl-201 and corrects for the decreasing spatial resolution with increasing distance from the pinhole aperture plane. Reconstructed activity is assumed to be at the center of each voxel. Sampling of the scintillation detector at  $128 \times 128$  matrix resolution introduces minimal resolution loss. Reconstruction time was 16 min (i.e., 1 min/plane) without hardware arithmetic.

**TABLE 2. LOCATION OF RECONSTRUCTED PLANES IN OBJECT SPACE**

Plane number	Distance from pinhole plane (cm)
-5	8.08
-4	8.56
-3	9.09
-2	9.70
-1	10.4
0	11.2
+1	12.2
+2	13.3
+3	14.6
+4	16.3
+5	18.3
+6	21.0
+7	24.6
+8	29.6

The *a priori* knowledge of a 2:1 myocardial-to-background ratio in the planar image was used to subtract background optimally from the raw planar image, in an attempt to improve its contrast and thus improve lesion detectability. The raw and background-subtracted planar images and the reconstructed tomographic images were quantitatively analyzed by a profile program to determine the defect-to-normal wall ratios in each image. Each profile intercepted the normal wall, traversed the central cavity through the phantom's principal axis, and bisected the  $90^\circ$  defect segment. Four to six pixels, centered on the peaks for the normal wall or defect, were used for least-squares quadratic fitting to interpolate the peak count value for that wall. The count ratios for peak defect to peak normal wall were used as a measure of imaging performance for comparison between planar and tomographic imaging. A smaller defect-to-normal-wall ratio indicates higher image contrast.

The commercial algorithm used for seven-pinhole image reconstruction terminated after only one iteration of the reconstruction process. Kirch et al. have demonstrated that use of an impedance estimator to obtain a first approximation to the reconstructed planes produces more rapid convergence than traditional estimators (7). To test convergence speed, the commercial algorithm was modified to permit user entry of the number of iterations. The same calibration and phantom data were then reconstructed for up to ten iterations. The global difference between the original seven-pinhole data and ray-summing of the final planes was determined as a function of iteration number and expressed as the average error of reconstruction.

After this experimental work had been performed, an improved reconstruction algorithm<sup>†,‡</sup> became available. The original calibration and phantom data were reconstructed with the new algorithm, and the reconstructed planes analyzed by profile analysis as described above. Quantitative comparisons were then made between the reconstructed images to examine specific differences between the two commercial reconstruction algorithms.

To study the effects of different commercial instrumentation and reconstruction software, the myocardial phantom experiment was performed on several camera/computer systems. The activity distribution within the phantom and its position within the tank were identical to those previously described. Sixteen-plane reconstructions were computed and the plane of highest defect contrast (i.e., lowest ratio between defect and normal wall activity) was identified quantitatively by profile analysis. The tomographic results were then compared between instrument systems.

#### RESULTS

The planar phantom image is shown in Fig. 5. The

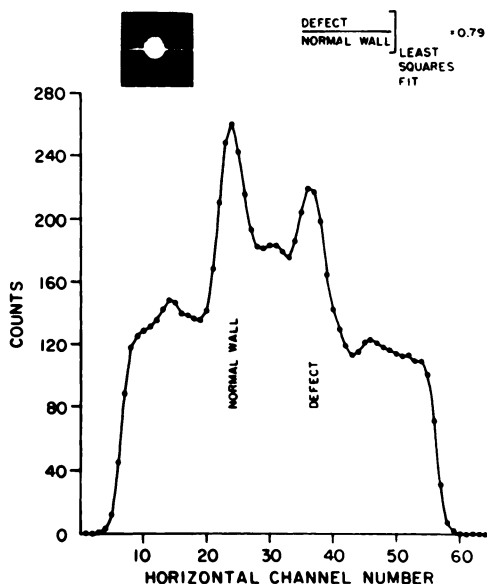


FIG. 5. Planar LAO image. Profile analysis bisecting planar image of phantom demonstrates 2:1 myocardium-to-background ratio for normal wall and shows ratio of 0.79 between defect and normal wall.

ratio of "normal" myocardial wall to extracardiac background is 2:1. Defect-to-normal-wall activity—as obtained by quadratic least-squares interpolation of the peak activity in opposing walls—was 0.79 for the 24-cc defect containing only water. *A priori* knowledge of the true background level permitted a 50% background subtraction to be made in an effort to enhance image contrast. The defect-to-normal-wall ratio following background subtraction was reduced to 0.70 (Fig. 6). The corresponding gray-scale image depicts higher

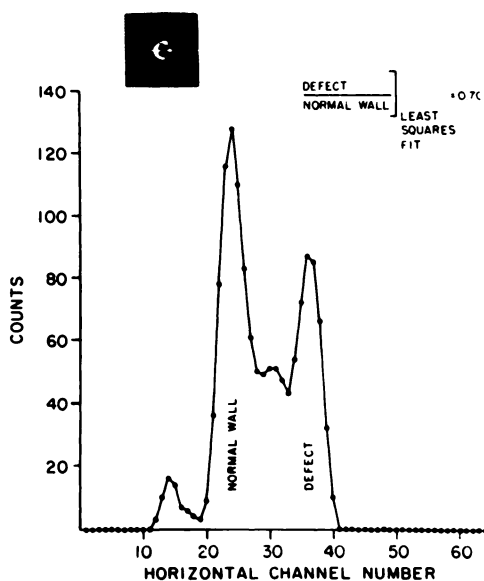


FIG. 6. Background-subtracted planar LAO image. From *a priori* knowledge of background ratio, 50% background subtraction merely reduced ratio between defect and normal wall to 0.70.

contrast (compare images in Figs. 5 and 6).

Tomographic images from apex (Plane -4) to base (Plane +4), calculated by the simultaneous iterative reconstruction algorithm\* are shown in Fig. 7. Visual assessment of the reconstructed images indicates a tomographic representation of the phantom's activity distribution. The defect sections of the phantom (Planes +2-+4) show a marked suppression of activity in the 24-cc chamber containing water. The presence of the small endocardial defect (at 11 o'clock) is perceived in these planes. Quantitative profile analysis through the normal wall and 24-cc defect segment is given in Fig. 7 for each image plane. In Planes +2-+4, which geometrically contain the defect, the profile through the defect falls to about half of the normal-wall activity, not to zero counts (i.e., below the in-plane background level), that would be expected for accurate tomography. In addition, the presence of the defect is seen quantitatively in most reconstructed planes proximal and distal to those that actually contain it. The plane of highest defect contrast (i.e., lowest ratio of defect-to-normal-wall activity) by least-squares interpolation of the peak activity in each wall is shown in Fig. 8. The minimum defect-to-normal-wall ratio was 0.54, not zero as it should be for a chamber containing no activity. The quantitative

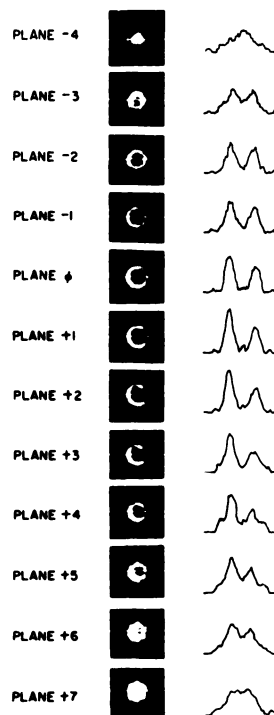
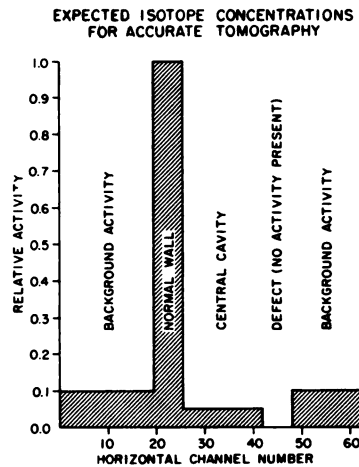
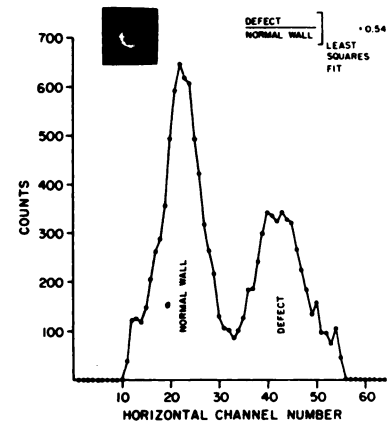


FIG. 7. Reconstructed images. Commercial algorithm\* was used to reconstruct raw data into longitudinal planes parallel to pinhole plane. Images progressing through phantom give visual impression of tomography. 5-cc fixed endocardial defect (Plexiglass plug) at 11 o'clock is detected in Planes +2 and +3. On high-quality video display, 1/8 in. spacers used to separate chambers in mid portion of phantom are also seen in these planes. 24-cc defect segment at 3 o'clock is clearly visualized.

**FIG. 8.** Quantitative evaluation of reconstructed images. Reconstructed plane showing highest contrast (lowest ratio of defect to normal-wall activities) is shown in right panel. Left panel defines true relationships. If reconstruction were accurate, defect (clean water) should fall below extracardiac background.



TOMOGRAPHIC SLICE (PLANE +3) WHICH SHOWS THE MINIMUM RATIO OF DEFECT TO NORMAL WALL (I.E., HIGHEST CONTRAST)



results are summarized in Fig. 9 and compared with the expected activity ratios for the reconstructed planes.

Convergence of the reconstruction algorithm for the phantom data is given in Fig. 10. The minimum-impedance estimator gives a good initial approximation to the reconstructed planes. After one iteration, when the commercial algorithm terminates, the reconstruction process is nearly converged. No significant differences in visual or quantitative analyses of the reconstructed images were apparent between the first and higher-order iterations.

A comparison of two commercial reconstruction algorithms is given in Fig. 11. Images and profiles of the same reconstructed plane are compared following reconstruction from the same calibration and phantom data. The present ADAC<sup>†</sup> algorithm is identical to the MDS<sup>||</sup> "MSET" program (D. M. Stern, private communication) and should produce results like those of Fig. 11, right panel, under the imaging conditions stated. (Also compare Fig. 12, center panel, with Fig. 11, right panel). Two major differences are observed in the corresponding planes of Fig. 11: (a) The CMS algorithm sets extracardiac background to zero, whereas the MDS/ADAC algorithm retains in-plane background; and (b) the spatial-frequency filter response of the CMS algorithm is higher, thus lowering the central cavity and defect activities relative to the "normal" wall activity and retaining slightly more random noise. These conclusions are portrayed both visually and quantitatively in Fig. 11.

The results of comparing seven-pinhole myocardial phantom imaging on several commercial tomographic systems are compared in Fig. 12. The most recent versions of the reconstruction algorithm were used, as is apparent from the in-plane extracardiac background activity and elevated central-cavity activity as previously discussed. The profiles across the reconstructed planes of highest defect contrast (i.e., minimum ratio of de-

fect-to-normal-wall activity) are portrayed. Reconstructed image quality and quantitative accuracy were similar among the three systems. All significantly overestimated the defect activity relative to the "normal" wall, and propagated the defect into reconstructed planes that contained no defect.

PROPAGATION OF THE DEFECT INTO RECONSTRUCTED SLICES OTHER THAN THOSE WHICH GEOMETRICALLY INTERSECT IT

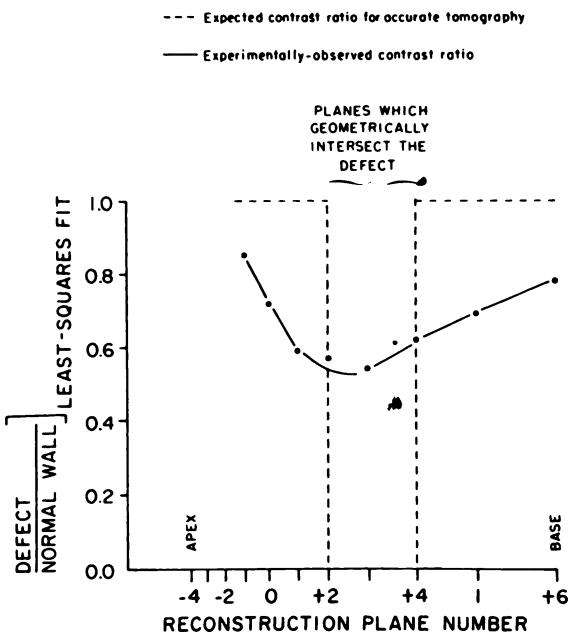


**FIG. 9.** Quantitative limitations of seven-pinhole tomography. Minimum contrast ratio for reconstructed planes that geometrically intersect defect (Planes +2-+4) is observed to be 0.54, not ideal zero. In addition, defect is shown by profile analysis to appear in most reconstructed planes. These quantitative inaccuracies most likely result from limited angle over which projection data are acquired by this technique.

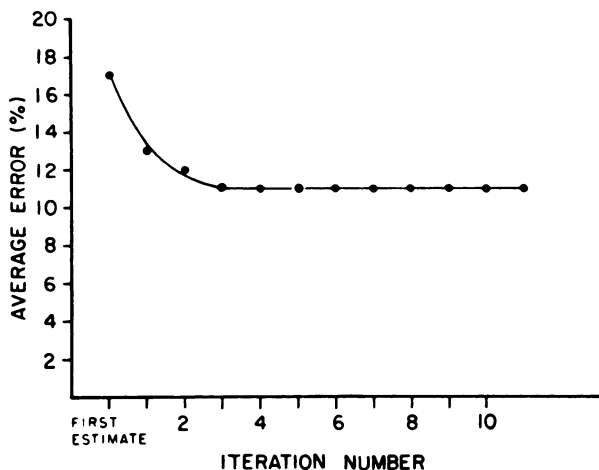


FIG. 10. Convergence of reconstruction algorithm. Same calibration and phantom data were reconstructed as function of iteration number. After one iteration (where all commercial algorithms terminate), reconstruction error is close to its asymptotic value. No significant difference was observed visually or quantitatively between images after one iteration as against three or more iterations of simultaneous iterative reconstruction technique.

DISCUSSION

Thallium-201 is currently the radionuclide of choice for studying relative myocardial perfusion. However, the presence of contiguous, noncardiac background activity, as well as the superposition of opposing or adjacent myocardial walls, has limited the clinical application of the technique. Additionally, absolute quantitation of thallium uptake has been impossible. Since tomographic approaches may circumvent the problem of superposition of structures and thus potentially allow quantitation, we studied seven-pinhole emission tomography with a cardiac phantom and the nuclide (thallium-201) currently used for cardiac perfusion studies, incorporating background thallium-201 in a tank that represented the thorax.

Under the imaging conditions specified, planar thallium myocardial imaging in the LAO view produced a defect-to-normal wall ratio of 0.79. Maximum background subtraction on the planar image increased the defect contrast and reduced the defect-to-normal-wall ratio to 0.70. Seven-pinhole tomographic imaging produced planes that visualized a tomographic presentation of the phantom's activity distribution from apex to base. In the reconstructed plane of maximum defect contrast, the defect-to-normal-wall ratio was 0.54, substantially lower than that obtained by planar imaging. Seven-pinhole tomography of the myocardial phantom system produced significantly higher image contrast, both visually and quantitatively, than did planar imaging, but it did not accurately reconstruct the phantom's cross-sectional activity distribution. The asymmetry of reconstructed contrast proximal and distal to the defect (Fig. 9) probably results from the decreasing spatial

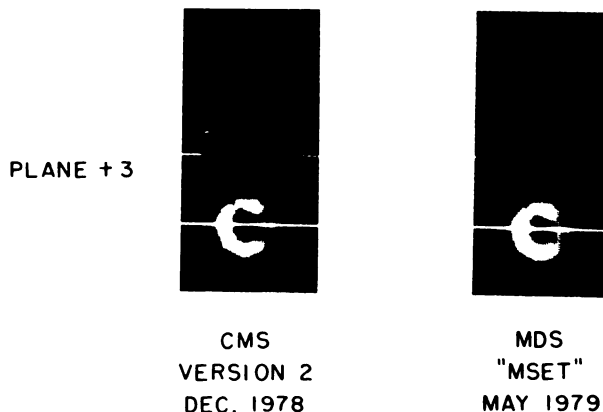


FIG. 11. Comparison of two reconstruction algorithms. Current ADAC and DEC Gamma 11 algorithms are identical to MDS program. Major differences are seen in extracardiac background, edge gradients, and random noise of reconstructed images. Same calibration and phantom data were used for these comparative reconstructions.

resolution with increasing distance from the pinhole plane (*l*).

Two quantitative artifacts were observed in the reconstructed planes. The defect's activity was grossly overestimated compared with activity in the normal wall (compare Fig. 8, right and left panels), and was propagated into planes proximal and distal to those in which it was actually situated (Fig. 7). The partial-volume effect, due to finite slice thickness, should not be a major contributor to these observations (8). Slice thickness is approximately one half of the longitudinal extent of the defect. Therefore, at least one of the three planes that intersected the defect should have completely intercepted its longitudinal extent. The most likely explanation for these artifacts is the lack of tomographic power (i.e., ability to separate superposed activity) resulting from the seven projections' limited angular coverage of the object's distribution.

A single defect, with 100% object contrast, was used in these experiments to study the imaging performance

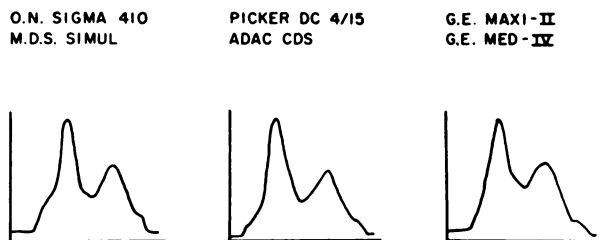


FIG. 12. Intercomparison of seven-pinhole tomography on several camera/computer/software systems. Phantom imaging, under conditions described in text, produced similar defect contrast in reconstructed images. Profiles intersect normal-wall and defect activities in reconstructed plane of highest defect contrast (minimum ratio between defect and normal-wall activities) for each imaging system.

in a simple controlled situation. A more complex object distribution might be defects of varying contrast and volume, located at different distances between the apex and base. Crosstalk between planes and the decreasing resolution with distance from the collimator, when taken in total, could result in adjacent defects' blurring together and in concentration averaging. Defects approaching a size equal to the spatial resolution may not be visualized due to inadequate contrast resolution or cross talk from adjacent regions of higher concentration.

It is well known that to reconstruct accurate cross sections of an object, the projections must cover a minimum of 180 degrees (9); and that a large number of projections within the angular coverage are necessary for a unique reconstruction (10). The theoretical limitations of limited-angle tomographic systems, including a point-source response calculation, have recently been discussed by Chiu et al. (11). In addition to adequate angular sampling, one must correctly address, in the reconstruction algorithm, the effects of digitizing resolution, the variation of spatial resolution with distance from the pinhole plane, finite pinhole aperture, and photon attenuation and scattering. The maximum-entropy reconstruction method of Minerbo (12) is a possible alternative to the simultaneous iterative reconstruction technique used by Vogel et al. (1).

The explanation of nonquantitative reconstruction is based on the central-slice theorem (13), which states that the Fourier transform of each projection determines a subset of Fourier coefficients at conjugate spatial frequencies in the Fourier representation of the object's cross section. Reconstruction can be described as inverse Fourier transformation of these coefficients. Accurate tomographic reconstruction results from determination of a complete set of Fourier coefficients (i.e., projections). The fundamental limitation on reconstruction accuracy for all limited-angle tomographic techniques is the lack of a complete set of the object's Fourier coefficients, because the total angle subtended by the projections falls short of the minimum 180° range necessary for accurate reconstruction (11). Some reduction of this inaccuracy may be achieved by analytic continuation, even in the presence of noise, as has been recently demonstrated by Inouye (14) and Tam et al. (15), and these methods may have applicability for improving the quantitative reconstruction accuracy in the seven-pinhole approach.

The minimum-impedance estimator, first used by Kirch et al. to obtain initial estimates of the reconstructed planes (7), produces rapid convergence of the reconstruction under the phantom conditions described here for myocardial imaging (see Fig. 10). Refinement of the initial planes by one iteration of the SIRT algorithm brings the average error close to its asymptotic value. Little difference was observed, visually or quan-

tatively, between the reconstructed planes after one iteration as against three or more. Thus, only a single iteration seems indicated—as is current practice in the commercially available reconstruction software.

Finally, when seven-pinhole myocardial tomography was simulated by phantom imaging on several combinations of wide-field computerized scintillation cameras with reconstruction software, all systems produced similar reconstructions. The quantitative results are summarized in Fig. 12 by profiles across the plane of highest defect contrast for each system. The results show consistency in the quantitative limitations discussed above, and indicate that similar results should be expected on available nuclear medicine instrumentation. While these phantom results indicate that seven-pinhole tomography offers improved image contrast within certain limitations imposed by the limited angular coverage of the object's distribution, a method of choice for clinical imaging should await the results of multicenter efficacy studies in which physiologic and anatomic variations are present.

#### FOOTNOTES

\* Cardiac Medical Systems, Inc., Northbrook, IL.

† ADAC, Inc., Sunnyvale, CA.

‡ Digital Equipment Corp., Maynard, MA.

§ Medical Data Systems, Inc., Ann Arbor, MI.

#### ACKNOWLEDGMENTS

Supported by the Medical Research Service of the Veterans Administration.

#### REFERENCES

1. VOGEL RA, KIRCH D, LEFREE M, et al: A new method of multiplanar emission tomography using a seven-pinhole collimator and an Anger scintillation camera. *J Nucl Med* 19: 648-654, 1978
2. LAKSHMINARAYANAN AV, LENT A: The simultaneous iterative reconstruction technique as a least-squares method. *SPIE Optical Instrumentation in Medicine V* 96: 108-116, 1976
3. VOGEL RA, KIRCH DL, LEFREE MT, et al: Thallium-201 myocardial perfusion scintigraphy: results of standard and multi-pinhole tomographic techniques. *Am J Cardiol* 43: 787-793, 1979
4. MUELLER TM, MARCUS ML, EHRHARDT JC, et al: Limitations of thallium-201 myocardial perfusion scintigrams. *Circulation* 54: 640-646, 1976
5. COOK DJ, BAILEY I, STRAUSS HW, et al: Thallium-201 for myocardial imaging: Appearance of the normal heart. *J Nucl Med* 17: 583-589, 1976
6. NARAHARA KA, HAMILTON GW, WILLIAMS DL, et al: Myocardial imaging with thallium-201: An experimental model for analysis of the true myocardial and background image components. *J Nucl Med* 18: 781-786, 1977
7. KIRCH DL, VOGEL RA, LEFREE MT, et al: An Anger camera/computer system for myocardial perfusion tomography using a seven-pinhole collimator. *IEEE Trans Nucl Sci* NS-27: 412-420, 1980

8. BROOKS RA, DICHIRO G: Slice geometry in computer assisted tomography. *J Comput Assist Tomogr* 1: 191-199, 1977
9. BUDINGER TF, GULLBERG GT: Three-dimensional reconstruction in nuclear medicine emission imaging. *IEEE Trans Nucl Sci* NS-21: 2-20, 1974
10. KATZ MB: *Questions of Uniqueness and Resolution in Reconstruction from Projections*. Berlin, Springer-Verlag, 1978
11. CHIU MY, BARRETT HH, SIMPSON RG, et al: Three-dimensional radiographic imaging with a restricted view angle. *J Opt Soc Am* 69: 1323-1333, 1979
12. MINERBO G: MENT: A maximum entropy algorithm for reconstructing a source from projection data. *Comp Graph Image Proc* 10: 48-68, 1979
13. MERSEREAU RM, OPPENHEIM AV: Digital reconstruction of multidimensional signals from their projections. *Proc IEEE* 62: 1319-1338, 1974
14. INOUE T: Image reconstruction with limited angle projection data. *IEEE Trans Nucl Sci* NS-26: 2666-2669, 1979
15. TAM KC, PEREZ-MENDEZ V, MACDONALD B: 3-D object reconstruction in emission and transmission tomography with limited angular input. *IEEE Trans Nucl Sci* NS-26: 2797-2805, 1979

## THE SOCIETY OF NUCLEAR MEDICINE 28th ANNUAL MEETING

**June 16-19, 1981**

**Las Vegas Convention Center**

**Las Vegas, Nevada**

### CALL FOR ABSTRACTS FOR SCIENTIFIC PROGRAM

The 1981 Scientific Program Committee solicits the submission of abstracts from members and nonmembers of the Society of Nuclear Medicine for the 28th Annual Meeting in Las Vegas, Nevada. Abstracts accepted for the program will be published in the June issue of the *Journal of Nuclear Medicine*. Original contributions on a variety of topics related to nuclear medicine will be considered, including:

**INSTRUMENTATION**

**COMPUTERS AND DATA ANALYSIS**

**IN VITRO RADIOASSAY**

**RADIOPHARMACEUTICAL CHEMISTRY**

**DOSIMETRY/RADIOBIOLOGY**

**CLINICAL SCIENCE/APPLICATIONS:**

Bone/Joint

Cardiovascular - Basic

Cardiovascular - Clinical

Cardiovascular - Peripheral Vascular

Endocrine

Gastroenterology

Hematology

Image Correlation

Infectious Disease and Immunology

Neurology

Oncology

Pediatrics

Pulmonary

Renal/Electrolyte/Hypertension

Only abstracts prepared on the official form will be considered. One official abstract form is required for each title submitted. Six copies plus supporting data (three pages maximum) attached to each copy must accompany the official abstract form. To ensure that all those interested in submitting abstracts receive the form, a copy of the official abstract form will be placed in the NOVEMBER issue of the JNM as a tear-out sheet. However, if you require additional forms, they may be obtained from the Society at the address below.

Abstracts of completed and on-going ("works in progress") projects will be judged together based on scientific merit.

Authors seeking publication for the full text of their papers are strongly encouraged to submit their work to the JNM for immediate review.

The official abstract form and six copies with supporting data attached to each copy should be sent to:

Society of Nuclear Medicine

ATT: Dennis Park

475 Park Avenue South

New York, NY 10016

Tel: (212) 889-0717

**DEADLINE FOR RECEIPT OF ABSTRACTS IS THURSDAY, JANUARY 8, 1981**